The FASEB Journal Express article fj.05-5547fje. Published online May 23, 2006.

The FASEB Journal • FJ Express Full-Length Article

Mechanism of nitric oxide action on inhibitory GABAergic signaling within the nucleus tractus solitarii

Sheng Wang,* Anja G. Teschemacher,† Julian F. R. Paton,* and Sergey Kasparov*,[1]

Departments of *Physiology and †Pharmacology, School of Medical Sciences, University of Bristol, Bristol, UK

ABSTRACT **The cellular mechanisms mediating nitric oxide (NO) modulation of the inhibitory transmission in the nucleus tractus solitarii (NTS) remain unclear, even though this could be extremely important for various physiological and pathological processes. Specifically, in the NTS NO-evoked glutamate and γ-aminobutyric acid (GABA) release might contribute to pathological hypertension. In cultured rat brainstem slices, NTS GABAergic neurons were targeted using an adenoviral vector to express enhanced green fluorescent protein and studied with a combination of patch clamp and confocal microscopy. Low nanomolar concentrations of NO increased intracellular Ca^{2+} concentration ($[Ca^{2+}]_i$) in somata, dendrites, and putative axons of GABAergic neurons, with axons being the most sensitive compartment. This effect was cGMP mediated and not related to depolarization or indirect presynaptic effects on glutamatergic transmission. Blockade of the cyclic adenosine diphosphate ribose (cADPR)/ryanodine-sensitive stores but not the inositol triphosphate-sensitive stores, inhibited NO effect. Since cADPR/ryanodine-sensitive stores are implicated in the Ca^{2+}-induced Ca^{2+} release, NO can be expected to potentiate GABA release. In support of this notion, a cADPR antagonist abolished the NO-induced potentiation of GABAergic inhibitory postsynaptic potentials in the NTS. Thus, the NO-cGMP-cADPR-Ca^{2+} pathway, previously described in sea urchin eggs, also operates in mammalian GABAergic neurons. Potentiation of GABA release by NO may have implications for numerous brain functions.—Wang, S., Teschemacher, A. G., Paton, J. F. R., Kasparov, S. Mechanism of nitric oxide on inhibitory GABAergic signaling within the nucleus tractus solitarii. *FASEB J.* 20, E000–E000 (2006)**

Key Words: ryanodine · cADPR · $[Ca^{2+}]_i$ · patch clamp

Nitric oxide (NO), a fascinating gaseous signaling molecule, has attracted the attention of numerous neuroscientists and has been implicated in a wide variety of brain functions, such as learning and memory, central autonomic control, neurodegeneration, and hormonal secretion, to name but a few. This laboratory has been focused for several years on the role of NO in central control of autonomic homeostasis with emphasis on the nucleus tractus solitarii (NTS). Indeed, the functional significance of NO signaling within the NTS has been well documented and particular attention has been paid to NO modulation of the baroreceptor reflex pathway, an action implicated in hypertension (for reviews see refs. 1, 2). However, attempts to clarify the actual role that NO plays in the NTS produced discordant results with some suggesting potentiation of the baroreflex (3–5), whereas others demonstrated either NO-mediated inhibitory actions (6–8) or no effect (9, 10). These differences might be attributable to a multiplicity of NO actions, including its ability to evoke both glutamate and γ-aminobutyric acid (GABA) release. Although the effects of NO on glutamatergic synapses have been studied extensively (11, 12; for reviews see refs. 13, 14), very little is known about its effects on inhibitory GABAergic transmission, although this could be at least as important for various physiological and pathological processes. Indeed GABAergic inhibition is fundamental for brain function and gets involved in all aspects of its activity. Overexpression of endothelial NO synthase (eNOS) in the rostral ventrolateral medulla led to elevation of extracellular concentrations of glutamate and GABA (15). Similarly, in striatum NO donors increased the release of both GABA and glutamate (16). However, the mechanism of these effects remains unknown and it is unclear whether NO-induced release of GABA results from a direct action on GABAergic neurons or an indirect effect via an increase in network activity driven by release of glutamate. To our knowledge, the most convincing evidence of a direct effect of NO on GABAergic neurons comes from the study by Li et al. (17), which demonstrated an increase in spontaneous GABAergic postsynaptic currents after application of an NO donor in the paraventricular nucleus of the hypothalamus (see also ref. 18).

NO could modulate GABAergic transmission by altering excitability of the GABAergic neurons (e.g., by depolarizing the membrane potential) or by a direct modulation of the transmitter release machinery. At presynaptic terminals, transmitter release is frequently regulated via changes in intracellular Ca^{2+} concentration ($[Ca^{2+}]_i$) either by modulation of external Ca^{2+}

[1] Correspondence: Department of Physiology, School of Medical Sciences, University of Bristol, Bristol BS8 1TD, UK. E-mail: sergey.kasparov@bristol.ac.uk

doi: 10.1096/fj.05-5547fje

influx or release from intracellular stores (10). Concerning the latter, the NO-cGMP pathway has been demonstrated to activate Ca^{2+} release from ryanodine-sensitive stores in sea urchin eggs (19) and glia (20). The NO-cGMP-Ca^{2+} pathway has also been implicated in the mechanisms of excitatory synaptic plasticity in the hippocampus (21, 22) and cerebellum (23). Whether these findings also apply to GABAergic transmission and to other areas of the brain is unknown. Therefore, we studied NO actions specifically on GABAergic inhibitory interneurons in the NTS. Specifically, we tested a hypothesis that NO has a direct effect on these neurons via an evolutionary conserved cGMP-cyclic adenosine diphosphate ribose (cADPR)-Ca^{2+} pathway, initially described in sea urchin eggs (19, 24, for review see ref. 25).

MATERIALS AND METHODS

Preparation of organotypic brainstem slice cultures

Slice cultures were prepared as described previously (26). Briefly, a Wistar rat pup (P8–10) was terminally anesthetized by halothane; the brainstem was dissected out and bathed in ice-cold dissection medium. Two-hundred and fifty micrometer thick slices containing the NTS were cut in cold (4°C) sterile dissection solution and then kept in dissection saline on ice for 1 h. Millicell-CM organotypic culture inserts (Millipore) were placed in sixwell culturing plates and moistened by addition of 1.0 ml OPTI–MEM based plating medium containing 30 μl adenoviral vector suspension to the side of each well. Two or three slices were deposited on each insert and the excessive medium was aspirated from the membrane surface. Slices were incubated at 37°C in a 5% CO_2 atmosphere. After 3 days, the plating medium was exchanged for Neurobasal-based culturing medium, which was subsequently exchanged twice a week. Slice cultures were allowed to settle for at least 7 days before being used for experimentation. For more details, including the composition of the media, see Teschemacher et al. (26).

The adenoviral vector used to visualize GABAergic neurons contains 3.7 Kb of GAD67 (glutamic acid decarboxylase) promoter sequence plus the first exon-intron sequence that drives expression of enhanced green fluorescent protein [enhanced GFP (EGFP); see also refs 26,27]. GAD67 is the key enzyme in the synthesis of GABA, and a shorter version of this sequence was used previously to target GABAergic neurons in a transgenic mouse (28). Thus, this vector induces expression of EGFP specifically in GABAergic neurons, which can be identified subsequently by fluorescence microscopy. This vector has different degrees of specificity in different areas of the brain, but in the NTS the absolute majority of EGFP-expressing neurons is immunopositve for GABA (26, 27), see also Supplementary Figs. 1 and 2.

Confocal imaging and electrophysiological recordings

All the imaging experiments were performed using a laser-scanning confocal microscope (SP-1 Leica) built on a fixed stage. A cultured slice was transferred to a glass bottomed chamber. The slice was superfused continuously with artificial cerebrospinal fluid (ACSF, see ref. 29 and in the experiments in acute slices described below) at 31 ± 1°C. For whole-cell patch clamp recordings, EGFP-expressing GABAergic interneurons were first identified in the NTS using conventional epifluorescence. The final stages of approaching the target neuron with a patch pipette (3–5 MΩ) and the formation of a seal were performed using the confocal scanner. The 488 nm wavelength line of the argon laser was used to excite EGFP, whereas the 633 nm Helium-Neon laser line was applied to obtain a differential interference contrast (DIC) image via a light detector located beneath the recording chamber. DIC optics greatly facilitated visualization of the slice surface and the pipette tip. Once the whole cell configuration was established, the identity of the patched neuron could be confirmed by the appearance of EGFP in the mouth of the patch pipette. Electrophysiological recordings were performed using the whole-cell mode. For Ca^{2+} imaging, cells were loaded with the Ca^{2+} indicator Rhod-2. The intracellular solution used in these experiments contained the following (in mM): 130 potassium gluconate, 10 HEPES, 5.5 EGTA, 4 NaCl, 2 $MgCl_2$, 1 $CaCl_2$, 2 ATP, 0.5 GTP, 5 glucose, and 0.5 of Rhod-2. Changes in $[Ca^{2+}]_i$ were assessed by relative fluorescence intensity (F/F_0, where F indicates peak fluorescence intensity and F_0 denotes resting fluorescence intensity). The Rhod-2 was excited using a green Helium-Neon laser line (543 nm), typically at levels of <0.5 mW, and Rhod-2-emitted light was sampled within the 560–640 nm band, as defined by the spectral scan head. In most cases, there was a big difference in fluorescence intensity between the soma, dendrite, and axon in the same image, and we therefore used two channels to sample Rhod-2 fluorescence (a low sensitivity channel for cell soma and a high sensitivity channel for neuronal dendrites and axons). This allowed us to obtain noiseless and unsaturated individual images of each cellular compartment.

No signs of any detrimental action of adenoviral vectors on neurons could be detected. Indeed, the EGFP-expressing neurons survived *in vitro* for weeks, essentially for as long as the slice culture remained viable. The morphology of the transduced cells is perfectly preserved; they demonstrate no swelling or segmentation of the soma or EGFP leakage. Electrophysiologically (resting membrane potential, spike amplitude, and membrane resistance) these neurons were similar to an "average" NTS neuron, as recorded in our previous studies using blind whole cell patch in acute NTS slices.

Electrophysiological recording in acute slices

Experiments were performed using brainstem slices of young rats (Wistar; postnatal days 12–15) prepared as described previously (29). Slices were placed into a conventional superfusion chamber, and neuronal recordings from the caudal NTS were made using the whole cell patch clamp configuration. Patch pipettes were filled with the same intracellular solution as described above but without Rhod-2 and containing 11 mM EGTA. The slices were superfused continuously with ACSF at a flow rate of 2 ml/min at 31 ± 5°C. Signals were amplified using a SEC-05LX amplifier (NPI), and the data were acquired and analyzed using Spike2 software (Cambridge Electronic Design).

Synaptic potentials were evoked by electrical stimulation via a concentric bipolar stimulating electrode (0.2 ms pulsewidth, 0.5–5 V, 0.3 Hz). When there was stimulation within the ipsilateral solitary tract, monosynaptic connections were apparent in <10% of neurons recorded, consistent with previously published observations (29–31). Therefore, to record monosynaptic inhibitory postsynaptic potentials (IPSPs), we applied 20 μM 6-cyano-7-nitroxaline-2,3-dione (CNQX, a blocker of non-NMDA receptor-mediated fast glutamatergic transmission), stimulated electrically within the central part of the NTS, and randomly searched for neurons

with CNQX-resistant IPSPs (typically 1 of 5–6 recorded cells, Supplementary Fig. 3). The evoked monosynaptic IPSPs had invariable latency ≤2 ms. IPSPs were recorded at holding potentials of −58 to −45 mV (those were kept unchanged for each individual cell for the duration of the recording) so that GABAergic events appeared hyperpolarizing. Because the EPSPs recorded in the medial NTS were mediated predominantly by non-NMDA receptors (30,31), only CNQX was used in this study to block polysynaptic connections. Indeed, 20 μM CNQX in our experiments completely blocked EPSPs in all cells where they were tested (data not shown). The recordings of evoked IPSPs commenced at least 10 min after whole-cell configuration was established. The amplitude of IPSPs at their peaks was measured from an average value for at least 10 consecutive IPSPs. According to previous data from our laboratory, IPSPs recorded in the NTS were in almost all cases sensitive to the $GABA_A$ receptor blocker bicuculline (32); therefore, in this study we assumed that they were mediated by $GABA_A$ receptors.

Drugs and their application

Diethylamine NONOate (DEA/NO) was dissolved in alkaline solution (10 mM NaOH) as concentrated stock solution and stored at −80°C. Thawing was allowed only before use when it was diluted into ACSF and used immediately. The half-life of DEA/NO at 37°C is 2 min and 16 min at 22–25°C in 0.1 M phosphate buffer (pH 7.4). DEA/NO, CNQX, ^{1}H-[1,2,4]oxadiazolo[4,3-a]quinoxalin-1-one (ODQ), nifedipine, 2-aminoethoxy diphenylborinate (2-APB), 8-bromo-cyclic adenosine diphosphate ribose (8-Br-cADPR), and tetrodotoxin (TTX) were purchased from Sigma. Rhod-2 (tripotassium salt) was supplied by Molecular Probes.

To estimate the actual effective concentration of NO at the recording site, we measured the real concentration of NO released by DEA/NO within the recording chamber using an electrochemical NO sensor (Amino-700, Innovative Instruments, see Supplementary Materials for more detail).

Statistical analysis

All values in this text are mean ± SE. Differences were examined using Student's paired *t* test, unpaired *t* test with Welch's correction, and one-way ANOVA with Post hoc Tukey's test, as appropriate and indicated in the text. $P < 0.05$ was considered significant. Statistical evaluation was carried out using Microsoft Excel and GraphPad Prism 4.

RESULTS

Initially we confirmed that both DEA/NO (see below) and aqueous solutions of NO (Supplementary Fig. 4) potentiate monosynaptic IPSPs in acute NTS slices. We therefore proceeded to investigate the possible mechanisms of NO effect on GABAergic neurons in organotypic slice cultures.

Effects of DEA/NO on NTS GABAergic interneurons in organotypic brainstem slice cultures

NTS GABAergic neurons transfected with adenoviral vector to express EGFP displayed a resting membrane potential of −58 ± 1 mV, input resistance of 195 ± 7 MΩ, and action potential amplitude of 85 ± 2 mV (n=57). Not only neuronal somata, but also dendrites and, in some cases, initial segments of axons could be visualized in Rhod-2-loaded cells (**Fig. 1**). The putative axons usually were <1 μM in cross-section and stemmed from a pyramid-like protrusions on the cell body (Fig. 1).

Effect of DEA/NO on $[Ca^{2+}]_i$ in GABAergic neurons

According to the measurements performed using the electrochemical NO sensor placed into the recording chamber of the confocal microscope, 1 and 10 μM DEA/NO generated 17 ± 7 and 121 ± 9 nM of NO (n=3 in both cases) in ACSF saturated with carbogen, (see Supplementary Materials). Application of 1 and 10 μM DEA/NO increased $[Ca^{2+}]_i$ in somata of GABAergic neurons in a concentration-dependent manner (**Fig. 2*A***). The DEA/NO-evoked rises in $[Ca^{2+}]_i$ were observed in almost all cells tested (n=5/5 for 1 μM, P<0.01; n=8/9 for 10 μM, P<0.01). $[Ca^{2+}]_i$ responses in eight cells treated with 10 μM DEA/NO developed at a latency of 17 ± 1 s and gradually increased over the next 0.3–5 min. Analysis of spatial distribution of fluorescence intensity revealed that although after bath application of 10 μM DEA/NO, $[Ca^{2+}]_i$ clearly increased in somata (+20±4%, n=9, P<0.01) and dendrites (+30±4%, n=9, P<0.001), the most dramatic increase occurred in the putative axons (+40±10%, n=6, P<0.05 compared with soma, ANOVA with

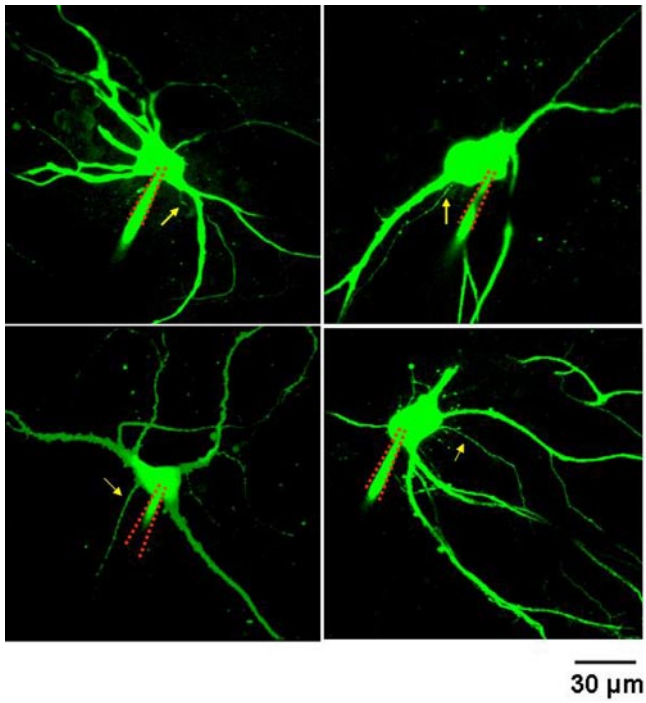

Figure 1. Rhod-2-loaded EGFP-expressing GABAergic neurons. EGFP-expressing GABAergic neurons in organotypic NTS slice cultures were loaded with Rhod-2 calcium sensitive dye from patch pipette. Images are maximum intensity projections of *x-y-z* confocal stacks displayed in pseudocolor. Dotted line and arrow indicate contour of patch pipette and putative axons, respectively.

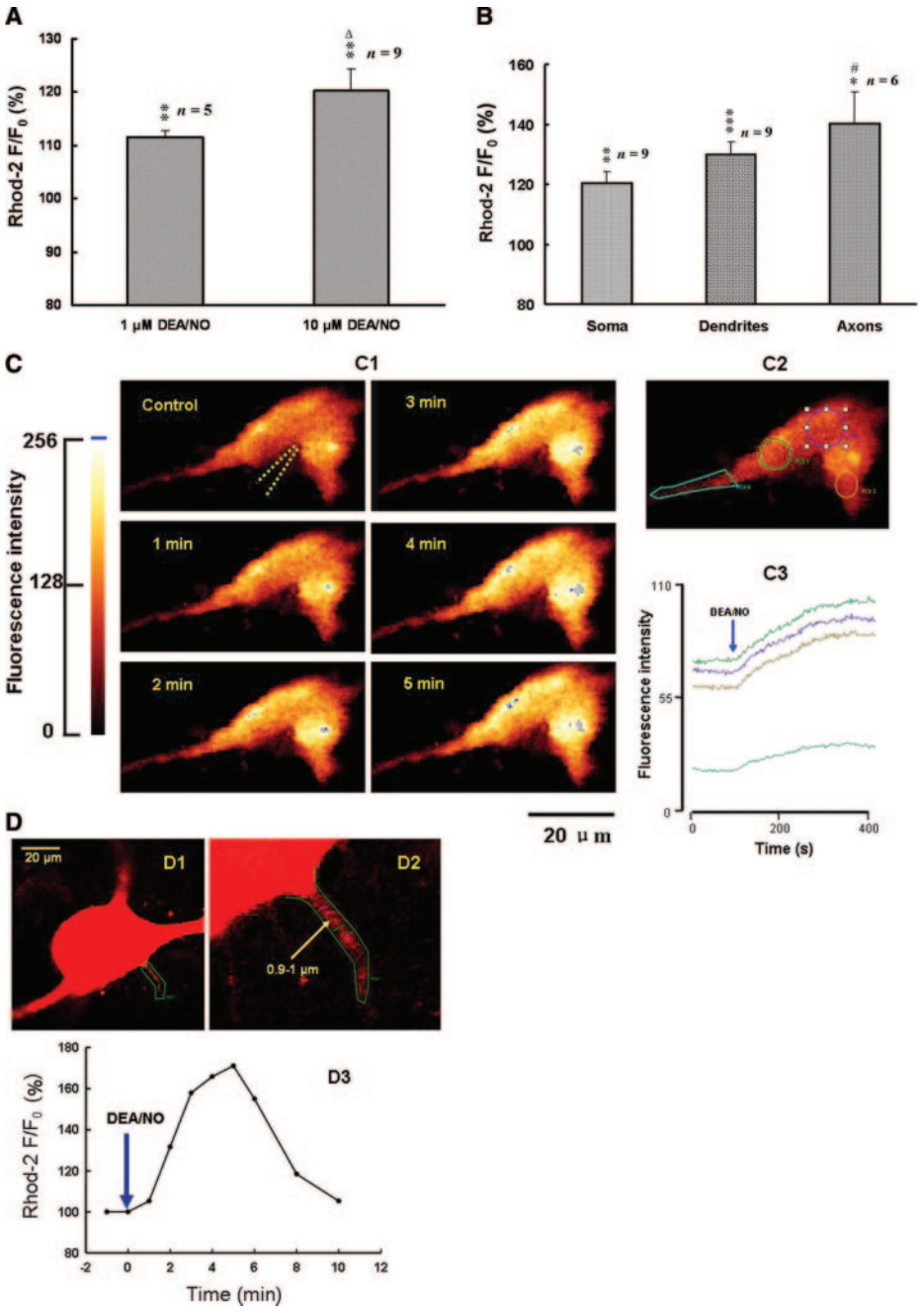

Figure 2. Effects of DEA/NO on $[Ca^{2+}]_i$ in different compartments of NTS GABAergic neurons. *A)* Bath application of both 1 and 10 μM DEA/NO elevated $[Ca^{2+}]_i$ as documented by a change in the relative fluorescence intensity of Rhod-2. *B)* 10 μM DEA/NO increases $[Ca^{2+}]_i$ in different compartments of GABAergic neurons. The most significant increase occurred in putative axons. *C)* An example of DEA/NO-induced elevation of $[Ca^{2+}]_i$ in a GABAergic NTS neuron. *C1)* Images taken from a time-lapse series to illustrate DEA/NO-evoked rises in $[Ca^{2+}]_i$. After application of DEA/NO different parts of neuron showed a progressive increase in brightness, as reflected by intensity-color palette (on *left*). Yellow dotted line in "Control" indicates profile of patch pipette. Color-intensity scale is shown on *left*; value of 256 corresponds to blue color. *C2)* In this neuron, several regions of interest were selected as depicted by shapes of different colors to measure fluorescence intensity. *C3)* DEA/NO-induced rises in fluorescence intensity reflect an increase in $[Ca^{2+}]_i$. Latency of this response is ≈15 s. DEA/NO-evoked $[Ca^{2+}]_i$ increases occurred in both the soma and dendrite. Blue arrow indicates beginning of infusion of 10 μM DEA/NO which continued until the end of this time lapse. *D)* DEA/NO increases $[Ca^{2+}]_i$ in a putative axon of a GABAergic neurone. *D1)* Initial segment of axon is visible in this GABAergic neurone shown in red pseudocolor. *D2)* An enlargement to illustrate axon shown in *D1*. Pyramid-like protrusion on membrane of cell can be identified at axonal hillock. Diameter of this putative axon is ≈0.9–1.0 μm. *D3)* Plot illustrating time course of DEA/NO-induced $[Ca^{2+}]_i$ increases. Bath application of 10 μM DEA/NO reversibly increased Rhod-2 F/F_0 in this axon. Arrow indicates moment of DEA/NO arrival into recording chamber, DEA/NO was discontinued after 5 min. $^*P < 0.05$, $^{**}P < 0.01$, $^{***}P < 0.001$, compared with control (paired *t* test). $^{\Delta}P < 0.05$, compared with the group treated with 1 μM DEA/NO, unpaired *t* test. $^{\#}P < 0.05$, compared with changes in soma, 1-way ANOVA with Tukey's test. Here and on all other figures 100% corresponds to values obtained before application of drugs.

Tukey's test; Fig. 2*B-D*). As axons could only be reliably visualized in some, but not all neurons, we have used $[Ca^{2+}]_i$ changes in somata for the data evaluation in this and the following sections. $[Ca^{2+}]_i$ elevations induced by DEA/NO in most cases were reversible and gradually declined within 5–10 min of washout.

Ten micromoles of DEA/NO also caused a moderate and reversible ODQ-sensitive depolarization in 66% (6 of 9) of the neurons (+3.4±1 mV, **Fig. 3*A***). However, depolarization occurred much later than the rises in $[Ca^{2+}]_i$ at a latency of 73 ± 9 s (Fig. 3*A-C*).

DEA/NO effect on $[Ca^{2+}]_i$ in GABAergic neurons is independent of synaptic transmission

To investigate whether the DEA/NO effect on GABAergic neurons is direct, a glutamate receptor inhibitor CNQX (20 μM) was used. In slice cultures pretreated

with CNQX for 10 min, the evoked rises in $[Ca^{2+}]_i$ (**Fig. 4*A*** and ***B***) and depolarization in five of six cells ($P < 0.05$, Fig. 3*B*) were unaffected after application of DEA/NO (10 μM). Thus, DEA/NO action is unlikely to result from glutamate release through polysynaptic connections. Moreover, bath application of 1 μM TTX also failed to prevent DEA/NO-induced increases in $[Ca^{2+}]_i$ (n=5, data not shown) and depolarizations (n=6, Fig. 3*C*), suggesting DEA/NO effects were not dependent on Na^+-dependent action-potential evoked transmitter release.

Membrane depolarization is not the reason for DEA/NO-induced $[Ca^{2+}]_i$ increases in GABAergic neurons

It was possible that DEA/NO-evoked depolarization could lead to transmembrane influx of extracellular Ca^{2+}, which could be registered as rises in $[Ca^{2+}]_i$. To test this hypothesis, membrane potential was depolarized using positive current injections by ≈5 mV (more than induced by 10 μM DEA/NO). Within 3 min, F/F_0 in soma increased by 10 ± 2% (n=5, P<0.05) and in dendrites by 14 ± 4% (n=5, P<0.05), which was significantly less than the changes seen after DEA/NO administration (**Fig. 5**, P<0.05, unpaired t test). The latency-to-onset of DEA/NO induced elevation of $[Ca^{2+}]_i$ (≈20 s) was shorter than that of the membrane depolarization (more than ≈1 min; compare Fig. 2*C* vs. Fig. 3*A*-C). In addition, DEA/NO-evoked $[Ca^{2+}]_i$ increases were observed in three cells that did not depolarize at all after DEA/NO administration. Finally, preventing depolarization by negative current injection in a small subset of neurons (n=2) did not prevent DEA/NO-evoked rises in $[Ca^{2+}]_i$ (data not shown). Therefore, DEA/NO-induced increases in $[Ca^{2+}]_i$ may not be directly attributed to membrane depolarization.

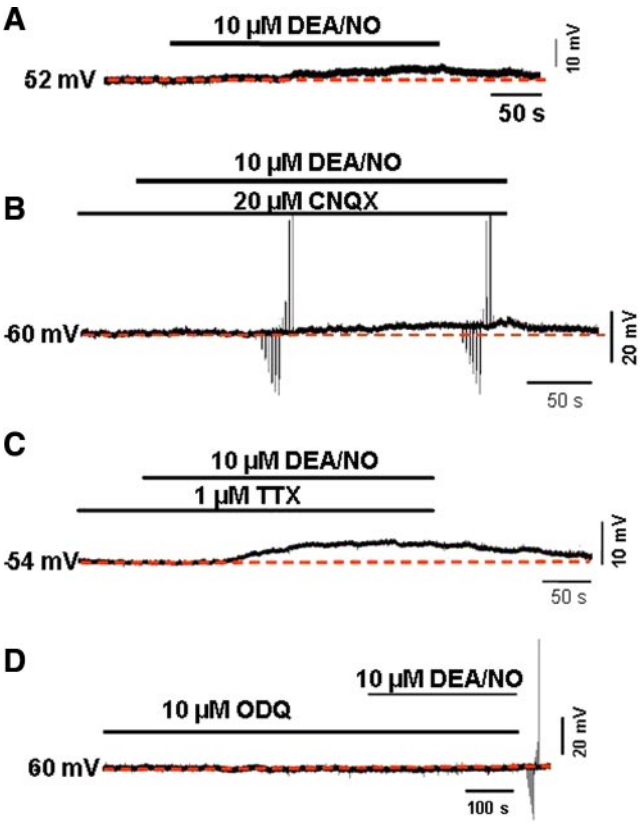

Figure 3. NO depolarizes some NTS GABAergic neurons. *A*) Bath application of 10 μM DEA/NO caused a reversible depolarization by ≈5 mV in an NTS GABAergic neuron. Latency of depolarization was >1.5 min, after arrival of DEA/NO into the chamber. *B)* In the presence of 20 μM CNQX, DEA/NO-induced depolarization was still observed, suggesting that glutamatergic non-NMDA receptors were not responsible for NO action. *C)* Pretreatment with 1 μM TTX failed to inhibit DEA/NO-induced depolarization, indicating that it was not dependent on fast Na^+ channels. *D*) DEA/NO-induced depolarization was abolished after combined perfusion of 10 μM ODQ and DEA/NO, indicating that this is a sGC-dependent effect. Action potentials were elicited by current injection delivered through the recording electrode at the end of the trace. Note that traces *A-D* are taken from different experiments.

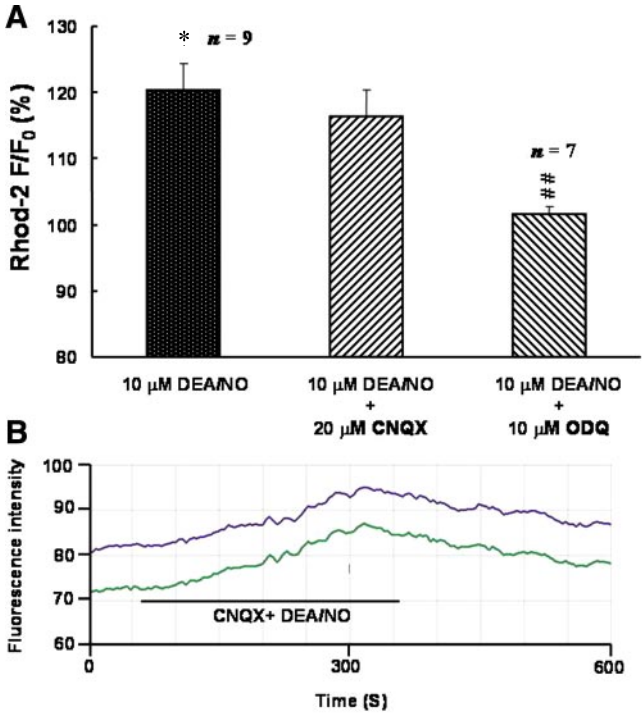

Figure 4. Cellular mechanisms underlying DEA/NO effects. *A)* DEA/NO-evoked $[Ca^{2+}]_i$ increases in GABAergic neurons persisted after administration of 20 μM CNQX (no significant difference between effects of DEA/NO and DEA/NO+20 μM CNQX). Thus, DEA/NO action is direct and not dependent on glutamatergic transmission. In contrast, application of 10 μM ODQ blocked DEA/NO-evoked $[Ca^{2+}]_i$ rises, indicating an involvement of sGC. *B)* DEA/NO-induced changes in fluorescence intensity from 2 regions of a soma of a GABAergic neuron in a typical experiment with application of CNQX. $^{**}P < 0.01$, compared with control (paired t test). $^{\#\#}P < 0.01$, compared with the group treated with DEA/NO alone, unpaired t test.

Effects of DEA/NO on GABAergic neurons are mediated by soluble guanylate cyclase

Soluble guanylate cyclase (sGC) is believed to mediate most of NO actions under physiological conditions. To

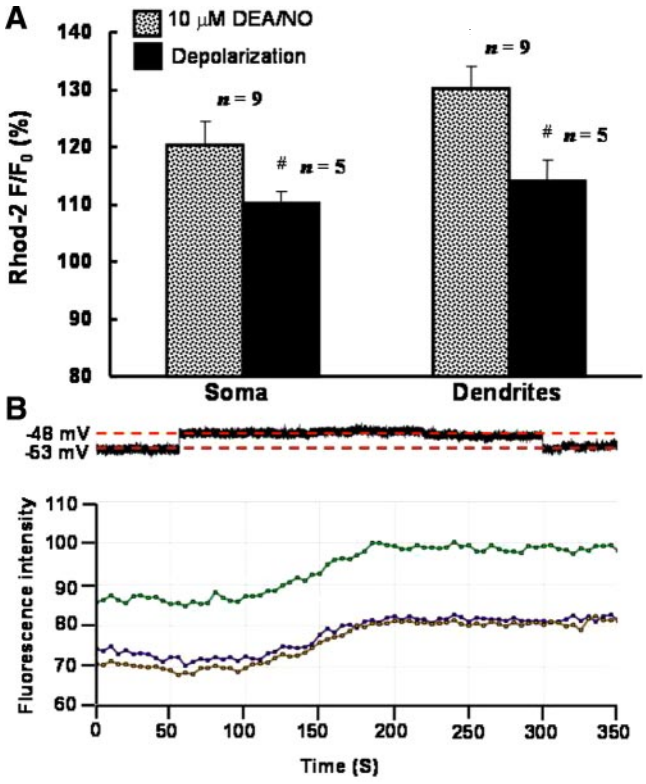

Figure 5. Depolarization may not account for DEA/NO-evoked $[Ca^{2+}]_i$ responses. In many cells, DEA/NO evoked membrane depolarization. To test whether DEA/NO-evoked $[Ca^{2+}]_i$ elevations were a result of depolarization, GABAergic neurons were depolarized by positive current injection by 4–5 mV, which is in excess of depolarization recorded after administration of 10 μM DEA/NO. *A)* Within 3 min, depolarization by current injection also induced an increase in $[Ca^{2+}]_i$ in soma and dendrites, but this was of significantly smaller amplitude compared with changes seen after DEA/NO administration. *B)* Effect of depolarization on $[Ca^{2+}]_i$ in soma (*upper trace*) and 2 dendrites of a GABAergic neuron in a typical experiment. $^*P < 0.05$, $^{**}P < 0.01$ $^{***}P < 0.001$, compared with control (paired *t* test). $^{\#}P < 0.05$, compared with group treated with DEA/NO alone, unpaired *t* test.

test whether it was involved in DEA/NO-induced rises in $[Ca^{2+}]_i$, the sGC antagonist ODQ (10 μM) was preperfused for 10 min, followed by combined perfusion with ODQ and 10 μM DEA/NO. Under these conditions, DEA/NO-evoked $[Ca^{2+}]_i$ rises and depolarization were completely abolished (n=6/7; Figs. 3*D* and 4*A*).

IP_3-sensitive stores are not the main source of DEA/NO-evoked $[Ca^{2+}]_i$ rises

Ten minutes of preincubation with 100 μM 2-APB, a blocker of IP_3-sensitive stores (33), were without effect on DEA/NO-evoked $[Ca^{2+}]_i$ increases in GABAergic neurons (n=5/6; P<0.01; **Fig. 6*A*** and Supplementary Fig. 5). Thus, IP_3-sensitive stores are unlikely to be the primary source of NO-released Ca^{2+}.

Nifedipine effect on DEA/NO-evoked $[Ca^{2+}]_i$ rises

Some data suggest that nicotinic acid adenine dinucleotide phosphate (NAADP) may operate an independent Ca^{2+} release mechanism (34) and that this pathway can be blocked by high concentrations (100 μM) of the L-type Ca^{2+} channel blocker nifedipine (35). Pretreatment with 100 μM nifedipine did not completely block DEA/NO action but reduced DEA/NO-induced $[Ca^{2+}]_i$ rises from 20 ± 4 to 12 ± 4% (n=4/5; P<0.05; Fig. 6*A*).

Blockade of ryanodine-sensitive stores by 8-Br-cADPR abolishes effects of DEA/NO

cADPR is thought to be an endogenous activator of ryanodine-sensitive Ca^{2+} stores (36–38). To test for the involvement of the cADPR/ryanodine-sensitive store, 8-Br-cADPR, a selective antagonist of cADPR, which has been reported to block cADPR-induced calcium release (39–41) but fails to block IP_3-sensitive stores (35), was introduced from the patch pipette (100 μM in the patch pipette solution). In the presence of 8-Br-cADPR, DEA/NO failed to evoke $[Ca^{2+}]_i$ elevations in seven of eight neurons. In addition, membrane depolarization was essentially abolished (+1±0.4 mV; n=8). Therefore, cADPR-sensitive Ca^{2+} stores are most likely to be the key link in the mechanism of NO action of GABAergic neurons (Fig. 6*A* and *B*).

2 NO-mediated potentiation of monosynaptic IPSP is mediated by cADPR

Having found that DEA/NO effects on $[Ca^{2+}]_i$ in GABAergic neurons are mediated by cADPR, experiments were performed in acute brainstem slices to test whether cADPR also mediates potentiation of monosynaptic GABAergic IPSPs. The NTS neurons recorded in these experiments had characteristics essentially identical to those found in our previous studies (29), e.g., mean resting membrane potential of −61 ± 2 mV, mean input resistance of 363 ± 64 MΩ, and mean action potential amplitude of 85 ± 2 mV. The experiments were performed in the presence of CNQX to cancel potential effects related to NO acting via glutamatergic mechanisms. Monosynaptic IPSP evoked from the medial portions of NTS in the presence of CNQX had invariable latency ≤2 ms. As shown in **Fig. 7**, 1 μM DEA/NO (which, according to the electrochemical NO sensor, released ≈55 nM of NO, see Supplementary Materials) potentiated IPSPs by ≈32%. This effect was reversible (Fig. 7) and could be repeated after 10 to 15 min of wash (not shown). DEA/NO-induced IPSP potentiation was essentially abolished by pretreatment with 30 μM 8-Br-cADPR (Fig 7*A* and *B*; P<0.01 as compared with DEA/NO only group and not significantly different from control, P>0.05). Thus, NO potentiates monosynaptic GABAergic IPSPS via a cADPR-dependent mechanism.

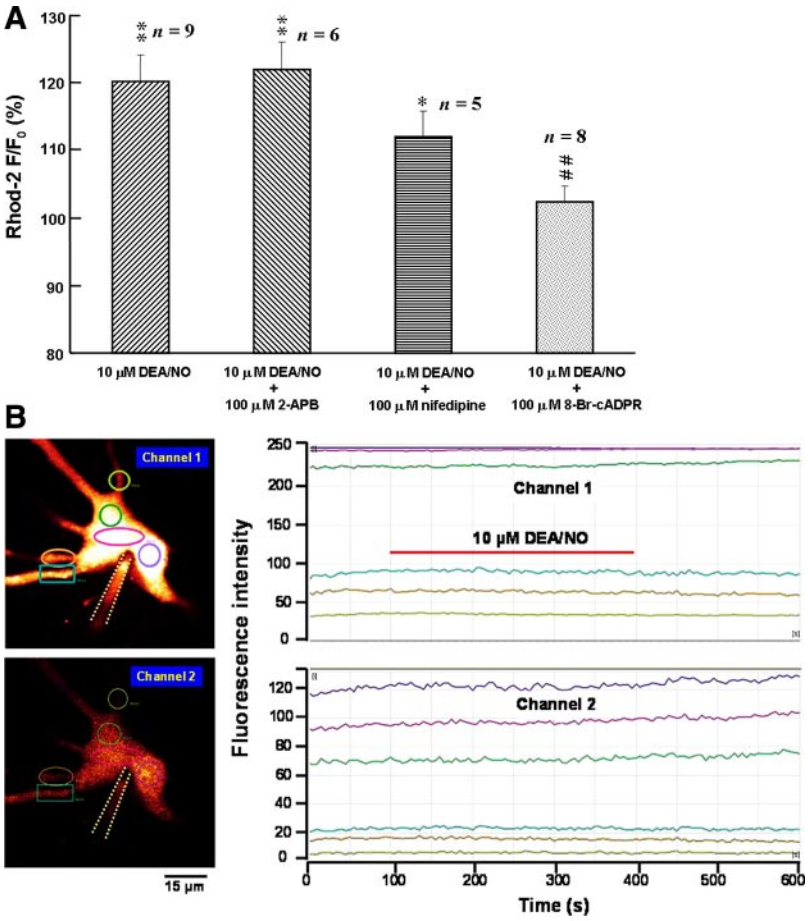

Figure 6. Calcium stores responsible for DEA/NO-induced $[Ca^{2+}]_i$ rises. *A, Left)* Effect of 10 μM DEA/NO shown for comparison. Pretreatment with 100 μM 2-APB (an inhibitor of the IP_3-sensitive Ca^{2+} release) failed to prevent DEA/NO effect; 100 μM nifedipine (a putative inhibitor of the NAADP-sensitive channel) did not block DEA/NO-elicited Ca^{2+} release, although there was a tendency to reduce it. Blockade of cADPR/ryanodine-sensitive stores with 8-Br-cADPR (a cADPR antagonist, 100 μM in patch pipette solution) abolished the effect of DEA/NO on Ca^{2+} release. Thus, cADPR/ryanodine-sensitive stores are likely to be the primary source of NO-released Ca^{2+} in GABAergic neurons. $^{*}P < 0.05$, $^{**}P < 0.01$, compared with control (paired *t* test). $^{\#\#}P < 0.01$, compared with group treated with DEA/NO alone, unpaired *t* test. *B)* cADPR/ryanodine-sensitive store appears to be responsible for DEA/NO-evoked $[Ca^{2+}]_i$ responses. Two channels were used to record changes in fluorescence intensity of soma and dendrites. Channel 1 was used to measure changes in dendrites (high sensitivity) and channel 2 for soma (low sensitivity). *Left panel)* Several areas of interest in soma and dendrites were chosen, as indicated by circle, rectangle, and ovals. Color-intensity palette is same as in Fig. 2*C*. *Right panel)* Traces show changes in fluorescence intensity of the chosen regions of the same neuron. In the presence of 8-Br-cADPR, DEA/NO failed to elevate $[Ca^{2+}]_i$ in both soma and dendrites. Note that confocal images are pseudocolor.

DISCUSSION

Our results lend support to the hypothesis of a direct stimulation of GABA exocytosis by NO and suggest that potentiation of Ca^{2+} release from cADPR/ryanodine-sensitive stores is the principal mechanism of NO-induced effect on the inhibitory transmission, at least in the NTS.

In brain tissue under normal conditions, NO originates predominantly from two sources: neuronal NOS and eNOS. In the intact brain, the enzymatic activity of NOS subtypes, their expression levels in different cellular compartments, sensitivity of glutamatergic and GABAergic neurons to NO, and the spatial relationships between the sources of NO and its targets would together determine the functional impact of NO-mediated signaling. Overall, the effective NO concentrations reported in our study are consistent with the EC_{50} values for activation of sGC by NO, which in different studies range from 20 to 45 nM (42) down to 2 nM (43) in intact brain cells.

NTS microinjections of the NO precursor L-arginine can induce baroreceptor reflex-like responses (i.e., falls in both arterial pressure and heart rate; refs 44, 45), whereas microdialysis of NO increased the extracellular concentration of glutamate consistent with facilitation of glutamatergic transmission (46, 47); this could account for the depressor/bradycardia noted above. On the other hand, chronic blockade of eNOS in the NTS increased baroreflex sensitivity (7), whereas both the NO donor and L-arginine depressed the baroreflex through an ODQ-sensitive mechanism in the working heart-brainstem preparation (6). The latter action strongly suggests that NO recruits an inhibitory mechanism in the NTS. Certainly, the GABAergic neurons are the obvious candidates for such a mechanism.

GABAergic inhibition is a fundamental feature of essentially any brain circuit, and therefore modulation of GABA release by NO must have far-reaching functional implications. Although the effects of NO on glutamatergic transmission have been studied extensively, there is no information about the mechanisms through which NO could modulate GABAergic transmission. Our study provides novel information to fill in this gap.

Ca^{2+} release from cADPR-ryanodine sensitive stores is a key element in NO action on GABAergic neurons

We have investigated the mechanisms of NO actions in organotypic slice cultured using an adenoviral vector to fluorescently label GABAergic neurons (26, 27). Neurotransmitter release depends on action potential-evoked influx of Ca^{2+} through voltage-operated channels, an effect amplified by Ca^{2+}-induced Ca^{2+} release from Ca^{2+}-dependent ryanodine-sensitive store. The latter can be modulated by cADPR, which makes it a

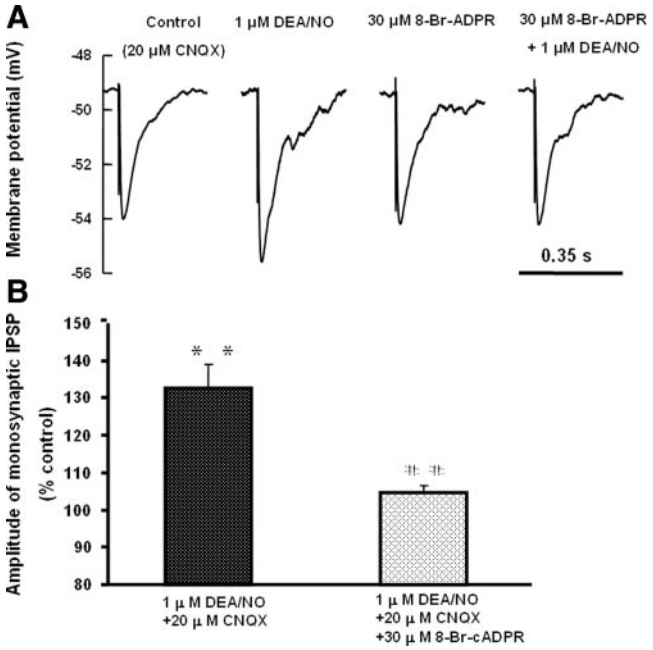

Figure 7. cADPR mediates NO-induced potentiation of monosynaptic IPSP. To test whether cADPR mediates the NO effect on GABA release, 8-Br-cADPR, an antagonist of cADPR, was bath-applied. *A)* In the presence of 20 μM CNQX, 1 μM DEA/NO increased the amplitude of IPSPs by ≈30%. After 15 min washout, bath application of 20 μM CNQX and 30 μM 8-Br-cADPR for 15 min, followed by addition of 1 μM DEA/NO. 8-Br-cADPR had no effect on IPSPs alone but abolished DEA/NO action (no significant difference compared with control in DEA/NO+8-Br-cADPR group). In preliminary experiments, we confirmed that the effect of DEA/NO is reproducible in the same cell after 10–15 min of wash (not shown). *B)* Pooled data illustrate that pretreatment with 8-Br-cADPR blocked the DEA/NO-induced potentiation of monosynaptic IPSPs in 5/5 cells. $^{**}P < 0.01$, compared with control (paired *t* test). $^{\#\#}P < 0.01$, compared with group treated with DEA/NO and CNQX only, unpaired *t* test.

good candidate for modulation by NO. In addition, even in the absence of Ca^{2+} influx, exocytosis can be stimulated by Ca^{2+} release from stores (48).

NO has been reported to increase $[Ca^{2+}]_i$ in sea urchin eggs (19) and rat parotid acinar cells (49). In cultured glial cells, micromolar concentrations of NO evoked Ca^{2+} release from ryanodine-sensitive stores (20). Consistent with these observations, nanomolar concentrations of NO increased $[Ca^{2+}]_i$ in GABAergic neurons in the present study (Fig. 2) This effect of NO was most dramatic in putative axons (Fig. 2*B* and *D*), suggesting that axonal release sites may be strongly modulated by NO. The factors responsible for the differential sensitivity of individual compartments may involve different concentrations of sGC, the potency of endogenous Ca^{2+} buffers, and spatial distribution of intracellular stores (reviewed in ref. 50). Our results could explain the recently reported NO donor-induced cGMP-mediated increase in the frequency of miniature GABAergic inhibitory postsynaptic currents in neurons of paraventricular nucleus (17). NO also potentiated [^{3}H]GABA release from primary neurons of mouse cerebral cortex through several mechanisms, including influx of external Ca^{2+}- and Na^+-dependent reversed GABA transporter (51, 52). However, these effects were to a large degree mediated by peroxynitrite, rather than cGMP. In contrast, all effects on GABAergic neurons in this study are cGMP-mediated, as ODQ completely eliminated both NO-induced $[Ca^{2+}]$ elevations and depolarization. Consistent with this notion, NO-induced cGMP accumulation in GABAergic fibers has been documented in the magnocellular nucleus of the hypothalamus (53). It must be acknowledged that although NO has been reported to trigger Ca^{2+} release from mitochondria in striatal neurons via a non-cGMP-dependent mechanism (54), the concentrations of NO used in that study were very high (4–10 μM), which is much higher than those used in our study.

cADPR is generated from NAD by ADP-ribosyl cyclase. cADPR binds to the same sites as ryanodine (discussed in refs. 50, 55) triggering Ca^{2+} release (56). In sea urchin eggs, cGMP mobilizes intracellular Ca^{2+} via stimulation of cADPR synthesis (24). The effects of NO on $[Ca^{2+}]_i$ in the present study were also cGMP-mediated and therefore could lead to activation of ADP-ribosyl cyclase, which is consistent with observations made in neurosecretory PC12 cells (57). Importantly, cADPR/ryanodine-sensitive stores are also responsible for the Ca^{2+}-induced Ca^{2+} release triggered by action potentials (36, for review see ref 50). Hence, the elevations in $[Ca^{2+}]_i$ reported here may be expected to boost the action-potential evoked Ca^{2+} transients and transmitter release, as found in the nodose ganglion cells (58) or neuroblastoma cell lines (59, 60). Whether the NO-cGMP-cADPR-Ca^{2+} pathway is sufficiently powerful to lead to action potential-independent GABA release is at present unclear, although some data suggest that this might be the case, at least in the hypothalamus (17). Our results provide a mechanistic explanation for the increase in the frequency of miniature GABAergic inhibitory postsynaptic currents in neurons of paraventricular nucleus reported in that study.

Here we directly demonstrate that potentiation of monosynaptic GABAergic IPSPs in the NTS depends on cADPR-mediated signaling, as its antagonist, 8-Br-cADPR, eliminates the effects of NO (Fig. 7). In these experiments, glutamatergic receptors were blocked with CNQX and therefore the effect of 8-Br-cADPR was mediated by its direct action on GABAergic neurons. It remains to be established whether activation of cADPR/ryanodine-sensitive stores also underlies the NO effects on glutamatergic transmission.

ADP-ribosyl cyclase also catalyzes conversion of NAD phosphate into NAADP. NAADP has been suggested to operate a separate Ca^{2+} channel in some cellular systems (61, 62). Thus, NO/cGMP/PKG/ADP-ribosyl cyclase cascade might be expected to have a NAADP-dependent component. In terms of our results, DEA/NO-induced $[Ca^{2+}]_i$ increases were to some extent inhibited by high concentrations of nifedipine (Fig. 6*A*), consistent with partial involvement of NAADP-sensitive store. However, more selective blockers are

needed to convincingly prove such a mechanism. Finally, we found no evidence for the involvement of IP_3-sensitive stores in the action of NO on GABAergic neurons (Fig. 6*A* and Supplementary Fig. 5) consistent with the mechanism originally described in sea urchin eggs (19).

It may be asked whether the depolarization triggered by DEA/NO in many GABAergic neurons could lead to Ca^{2+} entry through voltage-operated membrane channels, which could be registered as an increase in $[Ca^{2+}]_i$. We believe that this pathway has only a minor role, if any. First, NO-stimulated $[Ca^{2+}]_i$ rises were observed in some neurons without depolarization. Second, preventing depolarization by negative current injection in a small subset of neurons did not prevent $[Ca^{2+}]_i$ increases. Third, the latency-to-onset of elevations of $[Ca^{2+}]_i$ ($\approx$20 s) was much shorter than that of membrane depolarization (>1 min), indicating that Ca^{2+} is released before depolarization. Finally, although depolarization by current injection to the same concentration as that evoked by DEA/NO also increased $[Ca^{2+}]_i$ in the soma and dendrites, this increase was much smaller than the changes observed after DEA/NO administration (Fig. 5).

The effect on GABAergic neurons is direct, this conclusion being based on the experiments with CNQX to block AMPA receptors and TTX, which blocks action potentials and therefore the action potential-induced transmitter release (see "DEA/NO effect on $[Ca^{2+}]_i$ in GABAergic neurons is independent of synaptic transmission"). Indeed, TTX strongly inhibits release of neurotransmitters and must have suppressed or abolished any effects related to release of glutamate, including some potential unforeseen actions via metabotropic receptors. However, neither CNQX nor TTX had any clear effect on DEA/NO-induced Ca^{2+} elevations, which makes glutamate involvement highly unlikely.

Effects of NO on resting membrane potential

In our experiments, NO depolarized many GABAergic neurons in organotypic slice cultures and also unidentified NTS neurons in acute slices (data not shown). Depolarization of the GABAergic neurons could be abolished by a sGC inhibitor but not by a Na^+ channel blocker TTX or CNQX (Fig. 3), indicating that NO action is direct and not mediated by excitatory network interactions. NO-induced depolarization of GABAergic neurons and sensitization of Ca^{2+} stores in these cells may act synergistically to potentiate inhibitory transmission. Similar effects have been previously reported in several studies. In thalamic neurons, NO-induced depolarization resulted from a shift in activation of hyperpolarization-activated inward cationic conductance (63). Comparable effects were observed in paraventricular nucleus of hypothalamus (64), trigeminal motoneurons (65), and *Aplysia* central neurons (66). The mechanism underlying this depolarization is still unknown, but it has been proposed that cGMP modulates channel proteins via phosphorylation and/or dephosphorylation.

In conclusion, low nanomolar concentrations of NO may directly engage GABAergic inhibition via cGMP-mediated release of Ca^{2+} from axonal stores through an evolutionary conserved NO/cGMP/ADP-ribosyl cyclase/Ca^{2+} pathway. This effect may be assisted by membrane depolarization of some NTS GABAergic neurons and lead to the inhibitory NO actions seen at the systems level. FJ

Financial support from the Wellcome Trust (069061) and the British Heart Foundation (RJ/02/011) is gratefully acknowledged. S. Wang is an ORS award recipient.

REFERENCES

1. Paton, J. F. R., Kasparov, S., and Paterson, D. J. (2002) Nitric oxide and autonomic control of heart rate: a question of specificity. *Trends Neurosci.* **25,** 626–631
2. Paton, J. F. R., Deuchars, J., Wang, S., and Kasparov, S. (2005) Nitroxergic modulation in the NTS: Implications for cardiovascular function. In *Advances in Vagal Afferent Neurobiology* (Weinreich, D., ed.) Taylor & Francis Ltd and CRC Press pp. 209–246.
3. Maeda, M., Hirano, H., Kudo, H., Doi, Y., Higashi, K., and Fujimoto, S. (1999) Injection of antisense oligos to nNOS into nucleus tractus solitarii increases blood pressure. *Neuro. Report* **10,** 1957–1960
4. Talman, W. T., and Dragon, D. N. (2004) Transmission of arterial baroreflex signals depends on neuronal nitric oxide synthase. *Hypertension* **43,** 820–824
5. Hirooka, Y., Shigematsu, H., Kishi, T., Kimura, Y., Ueta, Y., and Takeshita, A. (2003) Reduced nitric oxide synthase in the brainstem contributes to enhanced sympathetic drive in rats with heart failure. *J. Cardiovasc. Pharmacol.* **42,** *Suppl.* 1, S111–S115
6. Paton, J. F. R., Ahmad, Z., Wong, L. F., Murphy, D., and Kasparov, S. (2001) Adenoviral vector demonstrates that angiotensin II-induced depression of the cardiac baroreflex is mediated by endothelial nitric oxide synthase in the nucleus tractus solitarii of the rat. *J. Physiol.* **531,** 445–458
7. Waki, H., Kasparov, S., Wong, L. F., Murphy, D., Shimizu, T., and Paton, J. F. (2003) Chronic inhibition of endothelial nitric oxide synthase activity in nucleus tractus solitarii enhances baroreceptor reflex in conscious rats. *J. Physiol.* **546,** 233–242
8. Matsumura, K., Tsuchihashi, T., Kagiyama, S., Abe, I., and Fujishima, M. (1998) Role of nitric oxide in the nucleus of the solitary tract of rats. *Brain Res.* **798,** 232–238
9. Pontieri, V., Venezuela, M. K., Scavone, C., and Michelini, L. C. (1998) Role of endogenous nitric oxide in the nucleus tratus solitarii on baroreflex control of heart rate in spontaneously hypertensive rats. *J. Hypertens.* **16,** 1993–1999
10. Zanzinger, J., Czachurski, J., and Seller, H. (1995) Effects of nitric oxide on sympathetic baroreflex transmission in the nucleus tractus solitarii and caudal ventrolateral medulla in cats. *Neurosci. Lett.* **197,** 199–202
11. Sistiaga, A., Miras-Portugal, M. T., and Sanchez-Prieto, J. (1997) Modulation of glutamate release by a nitric oxide/cyclic GMP-dependent pathway. *Eur. J. Pharmacol.* **321,** 247–257
12. Huang, C. C., Chan, S. H., and Hsu, K. S. (2003) cGMP/protein kinase G-dependent potentiation of glutamatergic transmission induced by nitric oxide in immature rat rostral ventrolateral medulla neurons in vitro. *Mol. Pharmacol.* **64,** 521–532
13. Talman, W. T., Dragon, D. N., Ohta, H., and Lin, L. H. (2001) Nitroxidergic influences on cardiovascular control by NTS: a link with glutamate. *Ann. N. Y. Acad. Sci.* **940,** 169–178
14. Esplugues, J. V. (2002) NO as a signalling molecule in the nervous system. *Br. J. Pharmacol.* **135,** 1079–1095
15. Kishi, T., Hirooka, Y., Sakai, K., Shigematsu, H., Shimokawa, H., and Takeshita, A. (2001) Overexpression of eNOS in the RVLM causes hypotension and bradycardia via GABA release. *Hypertension* **38,** 896–901
16. Trabace, L., and Kendrick, K. M. (2000) Nitric oxide can differentially modulate striatal neurotransmitter concentrations

via soluble guanylate cyclase and peroxynitrite formation. *J. Neurochem.* **75,** 1664–1674
17. Li, Y., Zhang, W., and Stern, J. E. (2003) Nitric oxide inhibits the firing activity of hypothalamic paraventricular neurons that innervate the medulla oblongata: role of GABA. *Neuroscience* **118,** 585–601
18. Stern, J. E., and Zhang, W. (2005) Cellular sources, targets and actions of constitutive nitric oxide in the magnocellular neurosecretory system of the rat. *J. Physiol.* **562,** 725–744
19. Willmott, N., Sethi, J. K., Walseth, T. F., Lee, H. C., White, A. M., and Galione, A. (1996) Nitric oxide-induced mobilization of intracellular calcium via the cyclic ADP-ribose signaling pathway. *J. Biol. Chem.* **271,** 3699–3705
20. Willmott, N. J., Wong, K., and Strong, A. J. (2000) A fundamental role for the nitric oxide-G-kinase signaling pathway in mediating intercellular Ca^{2+} waves in glia. *J. Neurosci.* **20,** 1767–1779
21. Reyes-Harde, M., Potter, B. V., Galione, A., and Stanton, P. K. (1999) Induction of hippocampal LTD requires nitric-oxide-stimulated PKG activity and Ca^{2+} release from cyclic ADP-ribose-sensitive stores. *J. Neurophysiol.* **82,** 1569–1576
22. Lu, Y. F., and Hawkins, R. D. (2002) Ryanodine receptors contribute to cGMP-induced late-phase LTP and CREB phosphorylation in the hippocampus. *J. Neurophysiol.* **88,** 1270–1278
23. Linden, D. J., Dawson, T. M., and Dawson, V. L. (1995) An evaluation of the nitric oxide/cGMP/cGMP-dependent protein kinase cascade in the induction of cerebellar long-term depression in culture. *J. Neurosci.* **15,** 5098–5105
24. Galione, A., White, A., Willmott, N., Turner, M., Potter, B. V., and Watson, S. P. (1993) cGMP mobilizes intracellular Ca^{2+} in sea urchin eggs by stimulating cyclic ADP-ribose synthesis. *Nature* **365,** 456–459
25. Guse, A. H. (2004) Regulation of calcium signaling by the second messenger cyclic adenosine diphosphoribose (cADPR). *Curr. Mol. Med.* **4,** 239–248
26. Teschemacher, A. G., Wang, S., Lonergan, T., Duale, H., Waki, H., Paton, J. F., and Kasparov, S. (2005) Targeting specific neuronal populations using adeno- and lentiviral vectors: applications for imaging and studies of cell function. *Exp. Physiol.* **90,** 61–69
27. Kasparov, S., Teschemacher, A. G., Hwang, D. Y., Kim, K. S., Lonergan, T., and Paton, J. F. (2004) Viral vectors as tools for studies of central cardiovascular control. *Prog. Biophys. Mol. Biol.* **84,** 251–277
28. Oliva, A. A., Jr., Jiang, M., Lam, T., Smith, K. L., and Swann, J. W. (2000) Novel hippocampal interneuronal subtypes identified using transgenic mice that express green fluorescent protein in GABAergic interneurons. *J. Neurosci.* **20,** 3354–3368
29. Kasparov, S., Paton, J. F. R. (1999) Differential effects of angiotensin II in the nucleus tractus solitarii of the rat-plausible neuronal mechanism. *J. Physiol.* **521,** Pt. 1, 227–238
30. Andresen, M. C., and Yang, M. Y. (1990) Non-NMDA receptors mediate sensory afferent synaptic transmission in medial nucleus tractus solitarius. *Am. J. Physiol.* **259,** H1307–H1311
31. Brooks, P. A., Glaum, S. R., Miller, R. J., and Spyer, K. M. (1992) The actions of baclofen on neurones and synaptic transmission in the nucleus tractus solitarii of the rat in vitro. *J. Physiol.* **457,** 115–129
32. Butcher, J. W., Kasparov, S., and Paton, J. F. (1999) Differential effects of apamin on neuronal excitability in the nucleus tractus solitarii of rats studied in vitro. *J. Auton. Nerv. Syst.* **77,** 90–97
33. Fernandez, S. F., Huang, M. H., Davidson, B. A., Knight, P. R., III, and Izzo, J. L., Jr. (2003) Modulation of angiotensin II responses in sympathetic neurons by cytosolic calcium. *Hypertension* **41,** 56–63
34. Genazzani, A. A., and Galione, A. (1996) Nicotinic acid-adenine dinucleotide phosphate mobilizes Ca^{2+} from a thapsigargin-insensitive pool. *Biochem. J.* **315,** Pt. 3, 721–725
35. Yusufi, A. N., Cheng, J., Thompson, M. A., Burnett, J. C., and Grande, J. P. (2002) Differential mechanisms of Ca^{2+} release from vascular smooth muscle cell microsomes. *Exp. Biol. Med. (Maywood)* **227,** 36–44
36. Hua, S. Y., Tokimasa, T., Takasawa, S., Furuya, Y., Nohmi, M., Okamoto, H., and Kuba, K. (1994) Cyclic ADP-ribose modulates Ca^{2+} release channels for activation by physiological Ca^{2+} entry in bullfrog sympathetic neurons. *Neuron* **12,** 1073–1079
37. Morrissette, J., Heisermann, G., Cleary, J., Ruoho, A., and Coronado, R. (1993) Cyclic ADP-ribose induced Ca^{2+} release in rabbit skeletal muscle sarcoplasmic reticulum. *FEBS Lett.* **330,** 270–274
38. White, A. M., Watson, S. P., and Galione, A. (1993) Cyclic ADP-ribose-induced Ca^{2+} release from rat brain microsomes. *FEBS Lett.* **318,** 259–263
39. Bruzzone, S. D. E. Flora, A., Usai, C., Graeff, R., and Lee, H. C. (2003) Cyclic ADP-ribose is a second messenger in the lipopolysaccharide-stimulated proliferation of human peripheral blood mononuclear cells. *Biochem. J.* **375,** 395–403
40. Chini, E. N., Nagamune, K., Wetzel, D. M., and Sibley, L. D. (2005) Evidence that the cADPR signaling pathway controls calcium-mediated microneme secretion in Toxoplasma gondii. *Biochem. J.* **389,** Pt. 2, 269–277
41. Teggatz, E. G., Zhang, G., Zhang, A. Y., Yi, F., Li, N., Zou, A. P., and Li, P. L. (2005) Role of cyclic ADP-ribose in Ca^{2+}-induced Ca^{2+} release and vasoconstriction in small renal arteries. *Microvasc. Res.* **70,** 65–75
42. Bellamy, T. C., and Garthwaite, J. (2001) Sub-second kinetics of the nitric oxide receptor, soluble guanylyl cyclase, in intact cerebellar cells. *J. Biol. Chem.* **276,** 4287–4292
43. Griffiths, C., Garthwaite, G., Goodwin, D. A., and Garthwaite, J. (2002) Dynamics of nitric oxide during simulated ischaemia-reperfusion in rat striatal slices measured using an intrinsic biosensor, soluble guanylyl cyclase. *Eur. J. Neurosci.* **15,** 962–968
44. Ohta, H., and Talman, W. T. (1994) Both NMDA and non-NMDA receptors in the NTS participate in the baroreceptor reflex in rats. *Am. J. Physiol.* **267,** R1065–R1070
45. Dias, A. C., Vitela, M., Colombari, E., and Mifflin, S. W. (2005) Nitric oxide modulation of glutamatergic, baroreflex, and cardiopulmonary transmission in the nucleus of the solitary tract. *Am. J. Physiol. Heart Circ. Physiol.* **288,** H256–H262
46. Lin, H. C., Kang, B. H., Wan, F. J., Huang, S. T., and Tseng, C. J. (2000) Reciprocal regulation of nitric oxide and glutamate in the nucleus tractus solitarii of rats. *Eur. J. Pharmacol.* **407,** 83–89
47. Matsuo, I., Hirooka, Y., Hironaga, K., Eshima, K., Shigematsu, H., Shihara, M., Sakai, K., and Takeshita, A. (2001) Glutamate release via NO production evoked by NMDA in the NTS enhances hypotension and bradycardia in vivo. *Am. J. Physiol. Regul. Integr. Comp. Physiol* **280,** R1285–R1291
48. Llano, I., Gonzalez, J., Caputo, C., Lai, F. A., Blayney, L. M., Tan, Y. P., and Marty, A. (2000) Presynaptic calcium stores underlie large-amplitude miniature IPSCs and spontaneous calcium transients. *Nat. Neurosci.* **3,** 1256–1265
49. Looms, D. K., Tritsaris, K., Nauntofte, B., and Dissing, S. (2001) Nitric oxide and cGMP activate Ca^{2+}-release processes in rat parotid acinar cells. *Biochem. J.* **355,** 87–95
50. Verkhratsky, A. (2005) Physiology and pathophysiology of the calcium store in the endoplasmic reticulum of neurons. *Physiol. Rev.* **85,** 201–279
51. Ohkuma, S., Narihara, H., Katsura, M., Hasegawa, T., and Kuriyama, K. (1995) Nitric oxide-induced [^{3}H] GABA release from cerebral cortical neurons is mediated by peroxynitrite. *J. Neurochem.* **65,** 1109–1114
52. Ohkuma, S., Katsura, M., Chen, D. Z., Narihara, H., and Kuriyama, K. (1996) Nitric oxide-evoked [^{3}H] gamma-aminobutyric acid release is mediated by two distinct release mechanisms. *Brain Res. Mol. Brain Res.* **36,** 137–144
53. Vacher, C. M., Hardin-Pouzet, H., Steinbusch, H. W., Calas, A., and De Vente, J. (2003) The effects of nitric oxide on magnocellular neurons could involve multiple indirect cyclic GMP-dependent pathways. *Eur. J. Neurosci.* **17,** 455–466
54. Horn, T. F., Wolf, G., Duffy, S., Weiss, S., Keilhoff, G., and MacVicar, B. A. (2002) Nitric oxide promotes intracellular calcium release from mitochondria in striatal neurons. *FASEB J.* **16,** 1611–1622
55. Galione, A., and Churchill, G. C. (2002) Interactions between calcium release pathways: multiple messengers and multiple stores. *Cell Calcium* **32,** 343–354
56. Galione, A., Lee, H. C., and Busa, W. B. (1991) Ca^{2+}-induced Ca^{2+} release in sea urchin egg homogenates: modulation by cyclic ADP-ribose. *Science* **253,** 1143–1146
57. Clementi, E., Riccio, M., Sciorati, C., Nistico G., and Meldolesi, J. (1996) The type 2 ryanodine receptor of neurosecretory PC12 cells is activated by cyclic ADP-ribose. Role of the nitric oxide/cGMP pathway. *J. Biol. Chem.* **271,** 17739–17745

58. Cohen, A. S., Moore, K. A., Bangalore, R., Jafri, M. S., Weinreich, D., and Kao, J. P. (1997) Ca^{2+}-induced Ca^{2+} release mediates Ca^{2+} transients evoked by single action potentials in rabbit vagal afferent neurones. *J. Physiol.* **499,** Pt. 2, 315–328
59. Empson, R. M., and Galione, A. (1997) Cyclic ADP-ribose enhances coupling between voltage-gated Ca^{2+} entry and intracellular Ca^{2+} release. *J. Biol. Chem.* **272,** 20967–20970
60. Hashii, M., Minabe, Y., and Higashida, H. (2000) cADP-ribose potentiates cytosolic Ca^{2+} elevation and Ca^{2+} entry via L-type voltage-activated Ca^{2+} channels in NG108–15 neuronal cells. *Biochem. J.* **345,** Pt. 2, 207–215
61. Clapper, D. L., Walseth, T. F., Dargie, P. J., and Lee, H. C. (1987) Pyridine nucleotide metabolites stimulate calcium release from sea urchin egg microsomes desensitized to inositol trisphosphate. *J. Biol. Chem.* **262,** 9561–9568
62. Lee, H. C., and Aarhus, R. (1995) A derivative of NADP mobilizes calcium stores insensitive to inositol trisphosphate and cyclic ADP-ribose. *J. Biol. Chem.* **270,** 2152–2157
63. Pape, H. C., and Mager, R. (1992) Nitric oxide controls oscillatory activity in thalamocortical neurons. *Neuron* **9,** 441–448
64. Bains, J. S., and Ferguson, A. V. (1997) Nitric oxide depolarizes type II paraventricular nucleus neurons in vitro. *Neuroscience* **79,** 149–159
65. Abudara, V., Alvarez, A. F., Chase, M. H., and Morales, F. R. (2002) Nitric oxide as an anterograde neurotransmitter in the trigeminal motor pool. *J. Neurophysiology* **88,** 497–506
66. Koh, H. Y., and Jacklet, J. W. (2001) Nitric oxide induces cGMP immunoreactivity and modulates membrane conductance in identified central neurons of Aplysia. *Eur. J. Neurosci.* **13,** 553–560

Received for publication January 17, 2006.
Accepted for publication February 27, 2006.